Available online at www.sciencedirect.com
ScienceDirect
Journal of Photochemistry and Photobiology A: Chemistry 184 (2006) 98–104
Journal of Photochemistry and Photobiology A:Chemistry
www.elsevier.com/locate/jphotochem

Formation of cytotoxic intermediates in the course of photodecomposition of a nitroheterocyclic antiseptic quinifuryl

Nasser A. Daghastanli [a], Igor A. Degterev [a,b], Gustavo B. Olivera [c], Amedea B. Seabra [d], Marcelo G. de Oliveira [d], Iouri E. Borissevitch [a,*]

[a] *Departamento de Física e Matemática, Faculdade de Filosofia Ciências e Letras de Ribeirão Preto, Universidade de São Paulo, Av. Bandeirantes 3900, Vila Monte Alegre, CEP 14040-901 Ribeirão Preto, SP, Brazil*
[b] *Department of Chemical & Biological Kinetics, Institute of Biochemical Physics, Russian Academy of Sciences, Kosygin Str. 4, 117333 Moscow, Russian Federation*
[c] *Departamento da Farmacologia, Faculdade da Medicina de Ribeirão Preto, Universidade de São Paulo, Av. Bandeirantes 3900, CEP 14040-901 Ribeirão Preto, SP, Brazil*
[d] *Instituto de Química, Universidade Estadual de Campinas, CP 6154, CEP 13083970 Campinas, SP, Brazil*

Received 9 January 2006; received in revised form 29 March 2006; accepted 1 April 2006
Available online 18 April 2006

Abstract

Phototoxicity of quinifuryl, 2-(5′-nitro-2′-furanyl)ethenyl-4-{*n*-[4′-(*n*,*n*-diethylamino)-1-methylbutyl]carbamoyl}quinoline, towards tumor cells has already been shown. Since no cytotoxicity of the final products of its photodecomposition was observed, we have supposed that cytotoxicity should be caused by reactive intermediates in the quinifuryl photolysis. We succeeded in detecting three species in the course of quinifuryl photolysis: singlet oxygen ($^1\Delta_g$), nitric oxide (NO) and superoxide anion ($O_2^{\bullet -}$). Singlet oxygen was detected by its specific phosphorescence in the course of the quinifuryl photoexcitation in both acetonitrile and aqueous solutions with lifetimes of 74.7 μs and 3.5 μs, respectively. The quantum yield of the $^1\Delta_g$ formation in water was 0.29 ± 0.03. Nitric oxide release was detected by specific chemiluminescence of excited radical $^*NO_2$, formed in the reaction of NO with O_3. The yield of NO was 0.45 ± 0.03 mol/mol of photodecomposed quinifuryl. The formation of $O_2^{\bullet -}$ was detected spectrophotometrically (epinephrine oxidation to adrenochrome) and by EPR (stable nitroxyl free radical formation).

Keywords: Quinifuryl photodecomposition; Cytotoxic intermediates; Superoxide anion free radical; Singlet oxygen; Nitric oxide

1. Introduction

Quinifuryl, 2-(5′-nitro-2′-furanyl)ethenyl-4-{*n*-[4′-(*n*,*n*-diethylamino)-1′-methylbutyl]carbamoyl}quinoline, 5-nitrofuranethenyl-quinoline (NFEQ) is known as an antiseptic agent [1], which possesses radiosensitizing activity in vitro [2] and cytotoxic activity towards various lines of tumor cells [3,4]. Recently, we have shown that phototoxicity of quinifuryl towards tumor cells, induced by visible light, was much higher as compared to its dark cytotoxicity [5,6]. It was also shown that the final products of quinifuryl photodecomposition are not toxic towards the same lines of tumor cells [6]. These results indicate that toxic intermediates formed in the course of the drug photolysis might be responsible for its photocytotoxicity.

We have also demonstrated previously that quinifuryl photodecomposition proceeds by two different pathways: the reaction between its molecules in the excited triplet and ground (S_0) states and the direct drug photodecomposition from the excited singlet state [7].

Further search for possible reactive intermediates of the quinifuryl photodecomposition was performed in the present work. Three potentially toxic intermediates of the drug photolysis by visible light (390–450 nm) were detected: singlet oxygen ($^1\Delta_g$), nitric oxide (NO) and superoxide anion ($O_2^{\bullet -}$).

* Corresponding author. Tel.: +55 016 3602 3862; fax: +55 016 3602 4887.
E-mail addresses: iourib@ffclrp.usp.br, iouribor@usp.br (I.E. Borissevitch).

1010-6030/$ – see front matter © 2006 Elsevier B.V. All rights reserved.
doi:10.1016/j.jphotochem.2006.04.004

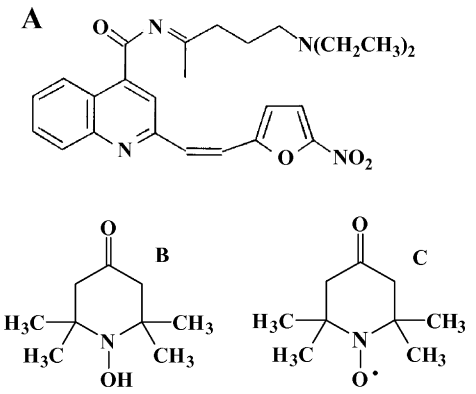

Fig. 1. Structure of quinifuryl (A), hydrophilic spin trap, 1-hydroxy-2,2,6,6-tetramethyl-4-oxopiperidine (TMOOP) (B) and the corresponding stable free nitroxyl radical (C).

2. Materials and methods

2.1. Chemicals

Quinifuryl (Fig. 1A), a representative of the family of 5-nitrofuran-ethenyl-quinoline drugs, was synthesized and purified by Dr. N.M. Sukhova (Institute of Organic Synthesis, Riga, Latvia). A hydrophilic spin trap, 1-hydroxy-2,2,6,6-tetramethyl-4-oxopiperidine (TMOOP), and the corresponding stable free nitroxyl radical (Fig. 1B and C), were synthesized and purified by Dr. L.A. Krinitskaya (Institute of Chemical Physics-RAS, Moscow, Russia). Acetonitrile, phenalenone and epinephrine were purchased from Merck and superoxide dismutase (SOD) was from Sigma Chemical Company. All reagents were used as received.

2.2. Quinifuryl photodecomposition measurements

Solutions of quinifuryl in phosphate buffer saline (PBS 7.5 mM, pH 7.8) were usually used, if not otherwise stated. The compound was irradiated by visible light in the spectral range from 390 nm to 450 nm using standard slide projector equipped with tungsten lamp (150 W). Light was passed through a color glass filter (5-57 KOPP, light transmittance range 350–450 nm). Irradiation was performed in a standard quartz cuvette with the 10 mm optical lengths. The initial solution absorbance at $\lambda_{max} = 396$ nm (characteristic quinifuryl absorption maximum) was always below 0.35. The irradiation intensity was 22 mW/cm^2, as measured at the front face of the sample cuvette by a Spectra-Physics 407A radiometer. A standard quartz cuvette (10 mm) filled with water was used as a thermal filter to prevent collateral heat effect. Quinifuryl photodecomposition was monitored through the decrease of absorption at 396 nm as described elsewhere [7]. Optical absorption spectra were registered using the DU 650 Beckman spectrophotometer. Solutions of quinifuryl were prepared using gentle stirring. Sample preparations were performed under light of 60 W red lamp, approximately 2 m from the light source, at controlled temperature (21 °C).

The effect of oxygen on quinifuryl photodecomposition was estimated by comparing the rate of the solvent absorbance reduction at 396 nm in open-to-air (aerated) and deaerated solutions. Deaeration was achieved by 40 min bubbling of quinifuryl solution with nitrogen before irradiation.

2.3. Singlet oxygen detection

A system consisting of a Nd:YAG Surelite III 1.0 laser linked to a dye laser was employed to excite quinifuryl ($\lambda_{exc} = 385$ nm). Measurements were performed in a standard quartz fluorescence cuvette in aerated 10–15 μM quinifuryl solutions in either acetonitrile or water. To detect the $^1\Delta_g$ formation, the phosphorescence was monitored in the spectral range from 1220 nm to 1310 nm using a modified spectrometer Edinburgh F900. The phosphorescence of the $^1\Delta_g$ was registered in acetonitrile quinifuryl solution, where $^1\Delta_g$ phosphorescence lifetime ($\tau_{^1\Delta_g}$) varied from 58 μs to 77 μs [8], and in water solutions, where $\tau_{^1\Delta_g}$ is between 2 μs [9] and 6 μs [10]. The quantum yield of $^1\Delta_g$ ($\Phi^{Q}_{^1\Delta_g}$) was measured in aqueous solution. To determine $\Phi^{Q}_{^1\Delta_g}$, the *meso*-tetrakis (*p*-sulfonatofenyl) porphyrin ($TPPS_4$, $\Phi^{P}_{^1\Delta_g} = 0.62$ [11]) was used as a standard. The $\Phi^{Q}_{^1\Delta_g}$ was calculated using the equation:

$$\Phi^{Q}_{^1\Delta_g} = \Phi^{P}_{^1\Delta_g} \frac{I_Q}{I_P} \frac{A_{P396}}{A_{Q396}} \quad (1)$$

where $\Phi^{Q}_{^1\Delta_g}$ and $\Phi^{P}_{^1\Delta_g}$ represent the quantum yields of $^1\Delta_g$ resulting from quinifuryl and $TPPS_4$ excitation, I_Q and I_P the $^1\Delta_g$ phosphorescence intensities at 1280 nm and A_{P396} and A_{Q396} are the absorbance of $TPPS_4$ and quinifuryl at 396 nm, respectively.

2.4. Superoxide anion ($O_2^{\bullet -}$) detection

Formation of $O_2^{\bullet -}$ in the course of quinifuryl photodecomposition was detected by two methods: epinephrine oxidation to adrenochrome [12] and the stable nitroxyl radical formation [13,14], both in the presence and in the absence of superoxide dismutase. In the epinephrine oxidation method 20 μM quinifuryl solution in PBS was irradiated in the presence of 1.1 mM epinephrine until complete quinifuryl photodecomposition. The absorption spectra were recorded in 300–600 nm spectral range as a function of the irradiation time. The quinifuryl photodecomposition and adrenochrome formation were monitored by the absorption decrease at 396 nm and its increase at 486 nm, respectively. Experiments were performed in the either absence or presence of oxygen. In the presence of oxygen experiments were performed either in the absence or in the presence of variable concentrations of SOD (10–100 units/ml).

The stable nitroxyl radical formation method is based on the formation of the stable free nitroxyl radical due to TMOOP oxidation by superoxide anion formed in the course of quinifuryl photodecomposition in the presence of oxygen. In these experiments 76 μM quinifuryl solution in PBS was irradiated in

the presence of 1.0 mM of TMOOP and after certain irradiation time intervals 100 μl of solution was inserted in a narrow gap (≈0.5 mm) EPR flat cell and the EPR spectrum was measured. The irradiation was continued until quinifuryl photodecomposition was completed (approximately 25 min). The solution of corresponding stable free nitroxyl radical (Fig. 1C) was used for calibration. These experiments were accompanied by the following controls: (a) the TMOOP solution was irradiated for 40 min without quinifuryl; (b) the solution containing both quinifuryl and TMOOP was incubated for 40 min in the dark; (c) the solution containing both quinifuryl and TMOOP was irradiated for 25 min in the presence of 16 μM SOD.

The EPR spectra were monitored at room temperature using the EPR spectrometer Varian E-4, X-band (9.47 GHz), 1 scan 3370–3390 G and 0.5 G modulation amplitude.

2.5. NO release detection

Release of free NO during the photolysis of aqueous quinifuryl solution was confirmed through the chemiluminescent NO detection.

In this test, liberation of NO was monitored by direct registration of chemiluminescence emitted by the NO_2 excited state (NO_2^*) formed in reaction of NO with ozone in the spectral region $\lambda > 600$ nm [15]:

$$NO + O_3 \rightarrow NO_2^* + O_2 \quad (2)$$

$$NO_2^* \rightarrow NO_2 + h\nu \quad (3)$$

Measurements were performed using an apparatus Sievers Model 280 equipped with an electrostatic ozone generator and a chemiluminescence reaction chamber (CRC) coupled with the NO Analyzer cube. The CRC is a ~20 ml reaction cell, where NO was mixed with ozone.

A calibration curve was obtained in the 0–300 pmol NO range using the reduction of $NaNO_2$ by 0.3 M sodium iodide solution in glacial acetic acid. NO released was transported to the CRC with a nitrogen flux where the chemiluminescence emission was measured. Integrated emission peaks (Fig. 2A) gave a linear correlation with NO_2^- concentration (Fig. 2B), expressed as 13.8 ± 2 mV s/pmol ($P < 0.0001$).

NO formation during quinifuryl photolysis was continuously measured until complete quinifuryl consumption detected by the disappearance of the chemiluminescence signal. The NO yield was calculated as:

$$\Phi_{NO}^{Q} = \frac{M_{NO}}{M_Q} \quad (4)$$

where M_{NO} and M_Q are the masses of the formed NO and consumed quinifuryl, respectively.

3. Results and discussion

3.1. Quinifuryl photodecomposition

Fig. 3A shows a representative spectral change associated with the photodecomposition of aqueous quinifuryl solution

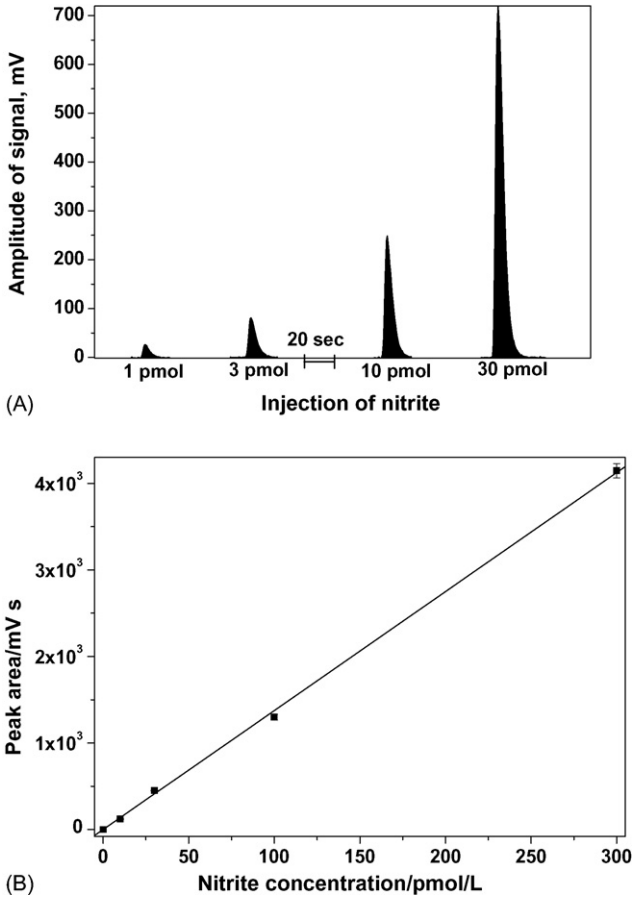

Fig. 2. (A) Luminescence peaks of NO_2^* formed in the reaction of NO with ozone after injection of various concentrations of NO-gas in the chemiluminescence chamber of a nitric oxide analyzer. (B) Dependence of the signal area on the quantity of injected •NO-gas (calibration curve).

with visible light. It can be seen that the main absorption band (with maximum at 396 nm) decreases continuously with irradiation. It was shown formerly that the absorption at 396 nm is assigned to π–π^* transitions of the nitrofuranoyl moiety [7]. Fig. 3B shows the normalized decay curves based on the 396 nm band obtained in aerated and deaerated solutions. It can be seen that the photobleaching of quinifuryl is faster in deaerated medium. Formerly it was demonstrated [7] that in addition to the unimolecular decomposition of quinifuryl from its exited singlet state (Q-$NO_2^*(S_1)$) (Eq. (5)), there is also evidence that Q-$NO_2^*(T_1)$ reacts with singlet quinifuryl molecules $Q(S_o)$. In accordance with [16] it is possible to suppose that final photoproducts can by formed via a transient radical species (Eq. (6)). In aerated solutions the probability of the last process is reduced due to the quinifuryl triplet quenching by molecular oxygen with the characteristic constant $k_q = 2.0 \times 10^9\ M^{-1}\ s^{-1}$. This value is close to the quenching constant characteristic for triplet energy transfer to oxygen, generating singlet oxygen ($^1\Delta_g$) (Eq. (7)) and suppressing the photodecomposition via Eq. (6).

$$Q\text{-}NO_2(S_o) + h\nu \rightarrow Q\text{-}NO_2^*(S_1) \rightarrow \text{Products} \quad (5)$$

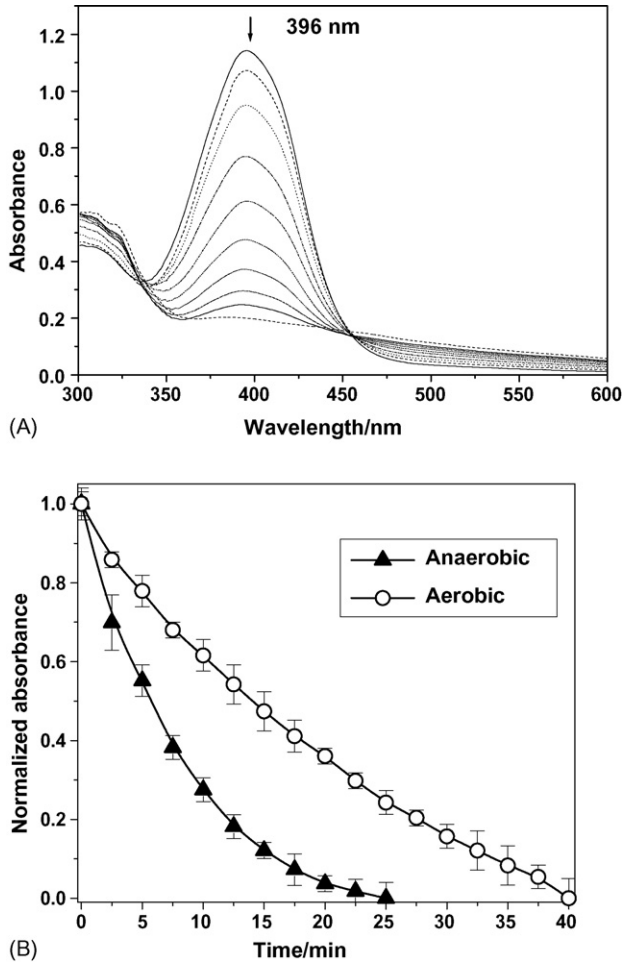

Fig. 3. Spectral changes (A) and kinetic curves (B) of quinifuryl photodecomposition based on the decrease of absorbance at 396 nm in the presence (◯) and in the absence (▲) of oxygen. Conditions: phosphate buffer (pH 7.8), photolysis by visible light (390–450 nm), room temperature.

$$\text{Q-NO}_2{}^*(\text{T}_1) + \text{Q-NO}_2(\text{S}_o) \rightarrow \text{Q-NO}_2{}^{\bullet-} + \text{Q-NO}_2{}^{\bullet+} \rightarrow \text{Products} \quad (6)$$

$$\text{Q-NO}_2{}^*(\text{T}_1) + \text{O}_2(\text{T}_1) \rightarrow \text{Q-NO}_2(\text{S}_o) + {}^1\Delta_g \quad (7)$$

3.2. Singlet oxygen formation

Fig. 4A shows the phosphorescence spectrum in the range 1220–1340 nm observed for quinifuryl in acetonitrile. A Gaussian fitting of this spectrum demonstrates that its maximum is localized near 1280 nm, which is characteristic of $^1\Delta_g$ phosphorescence [9,17]. The phosphorescence decay curves measured at 1280 nm, following the laser pulse excitation of quinifuryl dissolved in acetonitrile and water, are shown in Fig. 4B and C, respectively.

The rate of the $^1\Delta_g$ generation can be expressed as:

$$\frac{d[^1\Delta_g]}{dt} = k_q[T][O_2] - k_{^1O_2}[^1\Delta_g] \quad (8)$$

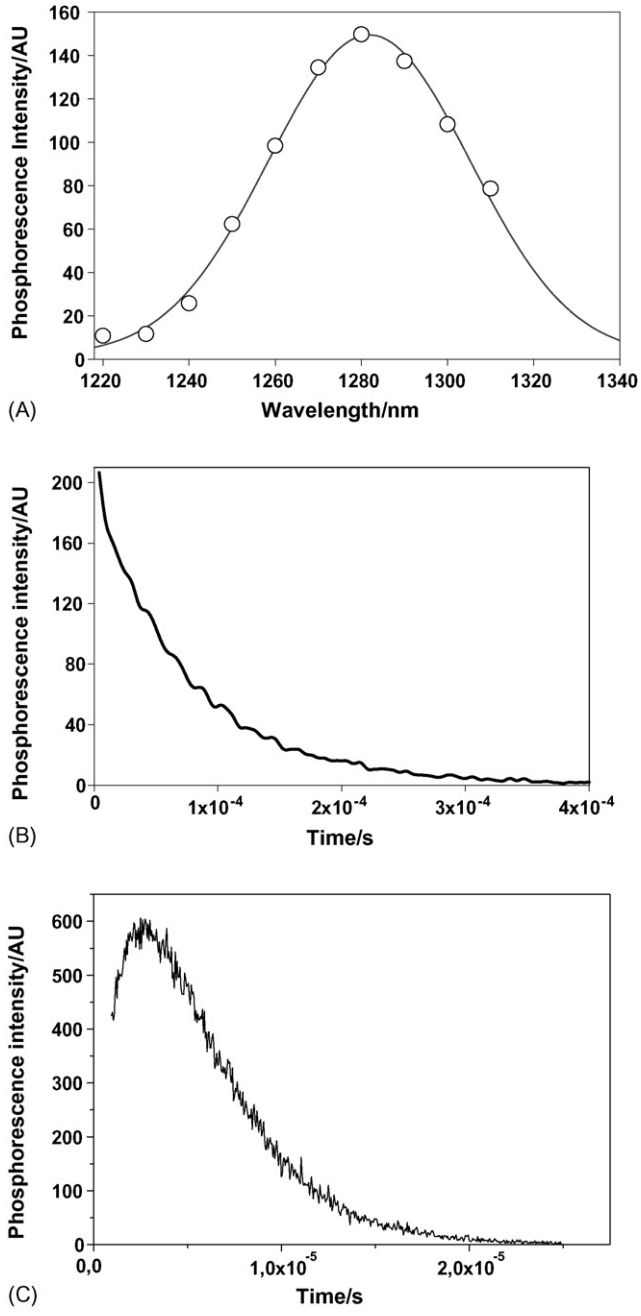

Fig. 4. The phosphorescence spectrum of $^1\Delta_g$ in acetonitrile (A) and phosphorescence decay curves at 1280 nm of the singlet oxygen ($^1\Delta_g$) produced due to the excitation of 20 μM quinifuryl by laser pulse at 375 nm in acetonitrile (B) and in water (C) solutions.

where k_q is the quenching constant of quinifuryl triplet by molecular oxygen and $k_{^1O_2}$ is the monomolecular decay constant of $^1\Delta_g$. Eq. (9) gives the changes of quinifuryl triplet state concentration as a function of time after the termination of the laser pulse.

$$[T] = [T_0]\exp[-(k_0 + k_q[O_2])t] \quad (9)$$

Since O_2 dissolved in water is about 10 times higher ($\sim 2.9 \times 10^{-4}$ M [18]) than quinifuryl (1–1.5×10^{-5} M; see Section 2), it is a good approximation to take O_2 concentra-

tion as constant throughout the reaction. The concentration of singlet oxygen can thus be written as

$$[^1\Delta_g] = \frac{k_q[O_2][T_0]}{k_{^1\Delta_g} - (k_0 + k_q[O_2])}\{\exp[-(k_0 + k_q[O_2])t - \exp(-k_{^1\Delta_g}t)]\} \quad (10)$$

where the first exponential term describes the accumulation of $^1\Delta_g$ due to the energy transfer from T to O_2, while the second exponential term is due to the $^1\Delta_g$ decay.

The $^1\Delta_g$ lifetimes calculated through the curve fittings of Fig. 4B and C in accordance with Eq. (10) were 74.7 μs and 3.5 μs for quinifuryl photoexcited in acetonitrile and aqueous solutions, respectively.

The quantum yield of $^1\Delta_g$ formation during quinifuryl photolysis in air-opened aqueous solutions ($\Phi^Q_{^1\Delta_g}$) was calculated according to Eq. (1) with $TPPS_4$ as a standard and was found to be $\Phi^Q_{^1\Delta_g} = 0.29 \pm 0.03$ ($P < 0.001$).

3.3. Superoxide anion formation

Irradiation of quinifuryl in the presence of epinephrine resulted in quinifuryl photodecomposition, evidenced by a decrease of absorbance at 396 nm, accompanied by the adrenochrome formation, monitored by an increase of absorbance at 486 nm (Fig. 5A), whose corresponding kinetic curves are shown in the inset. Current concentrations of both compounds were calculated using $\varepsilon_{396} = 2.47 \times 10^4\ M^{-1}\ cm^{-1}$ for quinifuryl [7] and $\varepsilon_{486} = 4.4 \times 10^3\ M^{-1}\ cm^{-1}$ for adrenochrome [19]. One can see that, while the rate of the quinifuryl photodecomposition increased in deaerated solution, compared to aerated one (2.5 ± 0.8 μM/min and 1.05 ± 0.2 μM/min, respectively; Fig. 3B), the rate of adrenochrome formation decreased sharply (from 6.4 ± 0.66 μM/min to 0.3 ± 0.5 μM/min; Fig. 5B) in deaerated solution. These results, along with the observation that no adrenochrome was detected when epinephrine was irradiated in aerated solutions in the absence of quinifuryl (data not shown), are an evidence that a reactive oxygen species (ROS), formed in the course of quinifuryl photolysis, was responsible for the epinephrine oxidation. The decrease in adrenochrome formation with SOD concentrations increase points to the formation of superoxide as a result of the quinifuryl photodecomposition. This can result from reaction between O_2 and a quinifuryl anion-radical, in a redox process, which can be represented as

$$Q\text{-}NO_2{}^*(T_1) + S \rightarrow Q\text{-}NO_2{}^{\bullet-} + S^{\bullet+} \quad (11)$$

$$Q\text{-}NO_2{}^{\bullet-} + O_2 \rightarrow Q\text{-}NO_2(S_o) + O_2{}^{\bullet-} \quad (12)$$

where S is a reductive substrate ($Q\text{-}NO_2(S_o)$ or epinephrine), similar to the photogeneration of $O_2{}^{\bullet-}$ described in other works [20–22].

The rate of quinifuryl photodecomposition was not significantly altered in the presence of either epinephrine (data not shown) or SOD (Fig. 5B), indicating that the bond cleavage in the nitro group is more probable due to the reaction between $Q\text{-}NO_2{}^*(T_1)$ and $Q\text{-}NO_2(S_o)$.

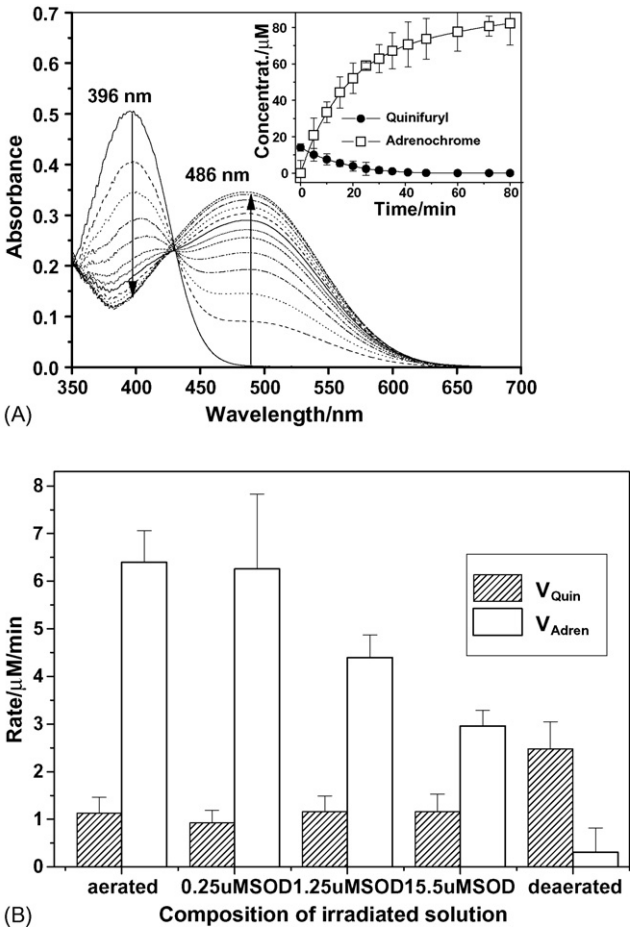

Fig. 5. (A) Spectral changes and kinetic curves (inset) of quinifuryl photodecomposition, based on the decrease in absorbance at 396 nm, and adrenochrome formation, based on the increase in absorbance at 486 nm. (B) Effect of oxygen and SOD concentration on the rates of photodecomposition of quinifuryl and the formation of adrenochrome. Conditions: all solutions were prepared in phosphate buffer saline, pH 7.8. [Epinephrine] = 1.1 mM, [quinifuryl] = 20 μM. Irradiation in the 390–450 nm spectral range at room temperature. Solutions were bubbled for 40 min with either oxygen (aerated) or nitrogen (deaerated) prior to irradiation. SOD was added to aerated solutions only.

Further confirmation of $O_2{}^{\bullet-}$ formation during quinifuryl photodecomposition in the presence of oxygen came from EPR measurements of the rate of stable nitroxyl free radical (NSFR) formation during quinifuryl photolysis in the presence of TMOOP (Fig. 6A). The kinetic curves of NSFR formation and quinifuryl consumption are presented in Fig. 6B. Kinetics of NSFR accumulation, measured in aerated and deaerated solutions containing quinifuryl and TMOOP, showed a reduction in the initial rate of the NSFR accumulation in deaerated solution (0.09 ± 0.08 μM/min), relative to aerated one (0.9 ± 0.08 μM/min) (Fig. 6C). This result demonstrates that oxygen is an important participant of NSFR formation from TMOOP in the course of quinifuryl photodecomposition and is strong evidence in favor of the generation of $O_2{}^{\bullet-}$. In addition, the kinetic curves of Fig. 6C also show that the rate of the NSFR formation decreased three times (from 0.9 ± 0.08 μM/min to 0.3 ± 0.08 μM/min) when quinifuryl was photolysed in aerated

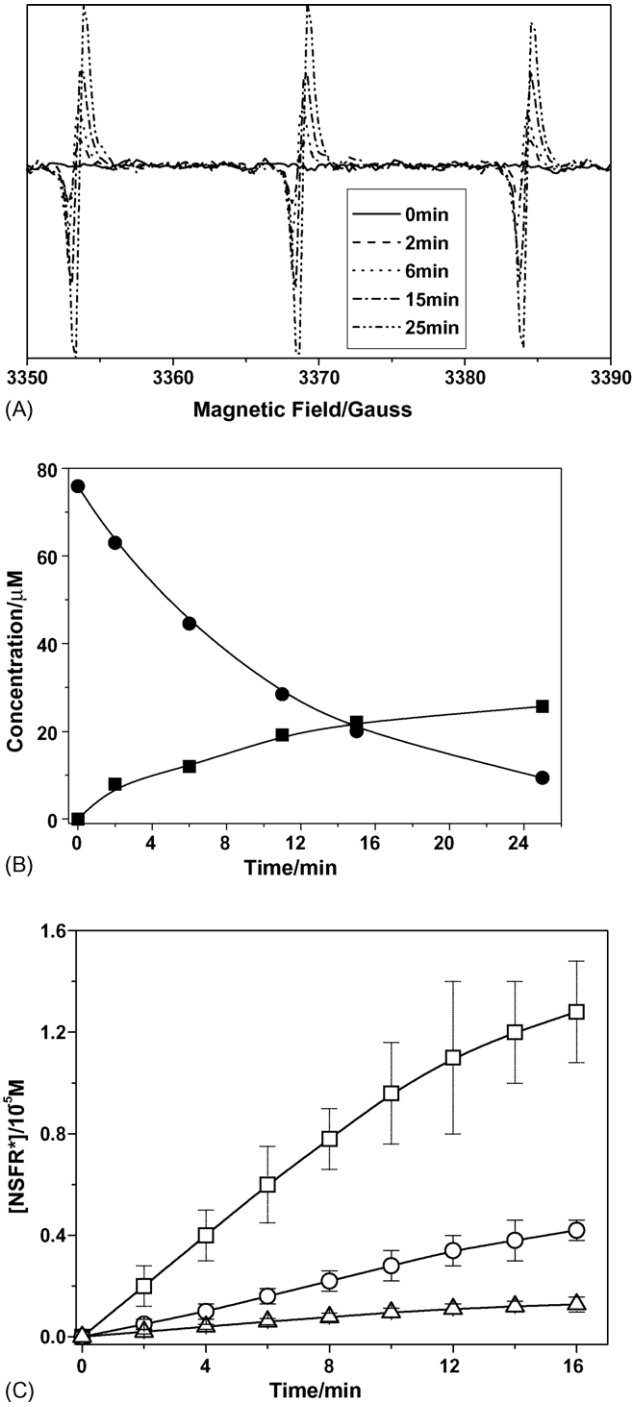

Fig. 6. (A) EPR spectra of the nitroxyl stable free radical (NSFR) formed in the course of the quinifuryl photodecomposition in the presence of TMOOP; (B) kinetic curve of NSFR formation (■) and quinifuryl consumption (●) in the course of irradiation; (C) kinetic curve of the NSFR accumulation in the course of quinifuryl photodecomposition in the presence of TMOOP in aerated solutions in the absence (□) or presence (◯) of SOD (15.2 μM) and in deaerated solutions (△).

solutions in the presence of 15.2 μM SOD. This result allows estimating that at lest 70% of the nitroxyl radicals were formed due to the reaction with $O_2^{\bullet -}$. The fact that no NSFR was detected when TMOOP was irradiated in aerated solution in the absence of quinifuryl (data not shown) reinforces the conclusion that $O_2^{\bullet -}$ formation is a result of quinifuryl photodecomposition in the presence of oxygen.

3.4. NO release

The release of free NO in the photodecomposition of quinifuryl was unequivocally demonstrated through the chemiluminescent signal obtained during the irradiation of the quinifuryl solution with visible light. The amount of NO released during the quinifuryl irradiation calculated from the calibration curve (Fig. 2A and B) was 60 ± 10 nmol. Compared to the initial amount of quinifuryl in the reaction flask (138 nmol) the amount of NO produced represents a reaction yield of 0.43 ± 0.07 mol NO/mol quinifuryl.

The photoejection of NO from quinifuryl (which can be represented here as RO–NO) can be assigned to the homolytic bond cleavage of the O–NO bond, forming two radicals: NO and $RO^{\bullet}$ (Eq. (13)). The fate of $R–O^{\bullet}$ radicals can be hydrogen abstraction from another quinifuryl molecule, forming an alcohol (R–OH, Eq. (14)) and leading to the propagation of the radical reaction, or dimerization (R–R, Eq. (15)). Of course, the formation of other secondary or tertiary more complex products in these processes cannot be ruled out.

$$RNO_2 \xrightarrow{h\nu} RO^{\bullet} + NO \quad (13)$$

$$RO^{\bullet} + RH \rightarrow ROH + R^{\bullet} \quad (14)$$

$$R^{\bullet} + R^{\bullet} \rightarrow R\text{-}R \quad (15)$$

Our previous studies have shown that quinifuryl possessed high cytotoxic activity towards a number of lines of cancer cells even in the dark [3,4,23,24]. This effect is due to reactive oxygen and nitrogen species, particularly, $O_2^{\bullet -}$ [14] and NO [25,26] produced in quinifuryl biotransformation. Elevated quinifuryl cytotoxicity under visible light irradiation, as compared with that in the dark, can be due to elevated NO, $O_2^{\bullet -}$ production and singlet oxygen formation, as well, whose cytotoxic activity is well documented [8,9]. The latter is not formed during quinifuryl biotransformation in the dark [5,6].

Moreover, since NO and $O_2^{\bullet -}$ are produced simultaneously, they can react in a diffusion-controlled process, forming anion peroxynitrite ($OONO^-$) [27]. Just a few drugs, such as 3-morpholino-sydnonimine (SN1) [28], doxorubicin (a quinone anthracycline antibiotic employed as anti-cancer agent), paraquat (1,1-dimethyl-4,4-bipyridinium dichloride) and 1-methyl-4-phenyl-1,2,3,6-tethrahydropyridine [29], are able to generate peroxynitrite, which in turn can react with carbon dioxide (CO_2) forming one more active species, an unstable nitrosoperoxycarbonate anion adduct ($O{=}N–OOCO_2^-$) [30]. $O{=}N–OOCO_2^-$ decomposes through homolytic cleavage, producing $^{\bullet}NO_2$ radical and carbonate radical anion ($CO_3^{\bullet -}$) [31]. $CO_3^{\bullet -}$ can diffuse from its site and propagate oxidative damage of biological targets [32], while $^{\bullet}NO_2$ can initiate free radical reactions by hydrogen abstraction from biological molecules [33].

Hence, we believe that the formation of singlet oxygen, NO, $O_2^{\bullet -}$ and subsequent generation of $OONO^-$ and

$O{=}N{-}OOCO_2^-$ species in the course of quinifuryl photolysis may explain its cytotoxic activity against tumor cells.

4. Conclusion

Photolysis of aqueous quinifuryl solutions with visible light produces at least three intermediate active species, nitric oxide ($^{\bullet}NO$), superoxide ($O_2^{\bullet -}$) and singlet oxygen ($^1\Delta_g$), which can lead to oxidative damage in cells and thus be responsible for the quinifuryl photocytotoxicity. The production of $^1\Delta_g$ in the course of quinifuryl photoactivation was demonstrated here for the first time. Moreover, the simultaneous production of NO and $O_2^{\bullet -}$ can promote peroxynitrite $OONO^-$ and anion $O{=}N{-}OOCO_2^-$ formation, inducing further increase of quinifuryl photocytotoxicity.

Acknowledgments

ABS held a graduate fellowship from Fundação de Amparo à Pesquisa do Estado de São Paulo (FAPESP), project 01/7869-9. The authors wish to thank FAPESP and CAPES for financial support.

References

[1] L.A. Blatun, A.M. Svetukhin, A.A. Pal'tsyn, N.A. Liapunov, V.A. Agafonov, Antibiot. Khimioter. (Mosc.) 44 (1999) 25–31.
[2] S.S. Voronina, N.K. Tatarskaya, I.A. Degterev, A.M. Serebrianiy, I.I. Pelevina, N.M. Sukhova, Radiobiol. (Mosc.) 25 (1985) 748–751.
[3] V.N. Verovskiy, I.A. Degterev, N.M. Sukhova, A.A. Buzukov, E.Yu. Leonova, N.K. Tatarskaya, Pharm. Chem. J. 24 (1990) 20–24.
[4] M.M. Rossa, T.A.A. Rocha-e-Silva, A.C. Tedesco, H.S.S. Araujo, I.E. Borissevich, I.A. Degterev, Pharm. Res. 48 (2003) 369–375.
[5] N.A. Daghastanli, M.M. Rossa, H.S. Selistre-de-Araujo, A.C. Tedesco, I.E. Borissevitch, I.A. Degterev, J. Photochem. Photobiol. B: Biol. 75 (2004) 27–32.
[6] N.A. Daghastanli, I.A. Degterev, A.C. Tedesco, I.E. Borissevitch, Braz. J. Med. Biol. Res. 37 (2004) 1873–1879.
[7] I.E. Borissevitch, N.A. Daghastanli, I.A. Degterev, J. Photochem. Photobiol. A: Chem. 159 (2003) 213–217.
[8] B.M. Monroe, Singlet oxygen in solutions: lifetimes and reaction rate constants, in: A.A. Frimer (Ed.), Singlet Oxygen. Physical–Chemical Aspects, vol. I, CRC Press, Florida, 1985, pp. 177–224.
[9] R. Bonnett, Chemical Aspects of Photodynamic Therapy. Advanced Chemistry Texts, vol. 1, Gordon and Breach Scientific Publishers, 2000, 39–56.
[10] D. Dolphin, Can. J. Chem. 72 (1994) 1005–1013.
[11] J. Mosinger, Z. Micka, J. Photochem. Photobiol. A: Chem. 107 (1997) 77–82.
[12] H.P. Misra, I. Fridovich, J. Biol. Chem. 247 (1972) 170–3175.
[13] Iu.E. Rashba, L.S. Vartanian, L.M. Baider, L.A. Krinitskaia, Biofizika (Mosc.) 34 (1989) 57–62.
[14] I.A. Degterev, A.A. Buzukov, N.K. Tatarskaya, E.Yu. Leonova, N.M. Sukhova, Pharm. Chem. J. 24 (1990) 9–16.
[15] P.M. Sievers (Ed.), Nitric Oxide Analyser (NOA 280). Operation and Service Manual. Software Version 2.05, Sievers, USA, 1997.
[16] V.A. Kuz'min, P.P. Levin, Yu.E. Borisevich, I.A. Degterev, S.M. Smirnov, Izvestia Acad. Nauk SSSR (Ser. Chem.) 24 (1988) 1510–1514.
[17] E. Cadenas, H. Sies, Low-level chemiluminescence as a indicator singlet oxygen in biological systems, in: H. Sies (Ed.), Oxygen Radicals in Biological Systems. Methods in Enzymology, vol. 105, Academic Press, San Diego, 1984, pp. 221–231.
[18] S.L. Murov, I. Carmichael, G.L. Hug (Eds.), Handbook of Photochemistry, second ed., M. Dekker, New York, 1993.
[19] M.J. O'Neil, A. Smith, P.E. Heckelman (Eds.), The Merck Index. An Encyclopedia of Chemicals, Drugs, and Biologicals, 13th ed., Merck & Co., Inc., Whitehouse Station, NJ, 2001, p. 33.
[20] Ye.N. Makareyeva, Ye.L. Lozovskaya, A.S. Tatikolov, I.I. Sapezhinskii, Biophysics 42 (1997) 461–467.
[21] K.K. Mothilal, J.J. Inbaray, R. Gandhidasan, R. Murugesan, J. Photochem. Photobiol. A 162 (2004) 9–16.
[22] K.R. Millington, G. Maurdev, J. Photochem. Photobiol. A 165 (2004) 177–185.
[23] I.A. Degterev, A.A. Buzukov, N.K. Tatarskaya, E.Yu. Leonova, N.M. Sukhova, Pharm. Chem. J. 24 (1990) 9–16.
[24] I.A. Degterev, A.A. Buzukov, V.G. Sharf, K.N. Popov, A.M. Serebrianiy, G.E. Zaikov, Pharm. Chem. J. 20 (1986) 412–417.
[25] V.B. Iliasova, A.A. Buzukov, M. Tabak, I.A. Degterev, Biophys. (Mosc.) 39 (1994) 219–225.
[26] A.A. Buzukov, V.B. Il'asova, M. Tabak, N.C. Meirelles, I.A. Degterev, Chem. Biol. Interact. 100 (1996) 113–124.
[27] G.C. Brown, V. Borutaite, Biochem. Biophys. Acta 1658 (2004) 44–49.
[28] R.J. Sing, N. Hogg, J. Joseph, E. Konorev, B. Kalyanaraman, Arch. Biochem. Biophys. 361 (1999) 331–339.
[29] A. Denicola, R. Radi, Toxicology 205 (2005) 273–288.
[30] R.M. Uppu, G.L. Squadrito, W.A. Pryor, Arch. Biochem. Biophys. 327 (1996) 335–343.
[31] A. Veselá, J. Wilhelm, Physiol. Res. 51 (2002) 335–339.
[32] D.C. Ramirez, S.E.G. Mejiba, R.P. Mason, J. Biol. Chem. 280 (2005) 27402–27411.
[33] J.C. Niles, J.S. Wishnok, S.R. Tannenbaum, Nitric Oxide 14 (2006) 109–121.